Published OnlineFirst January 21, 2014; DOI: 10.1158/0008-5472.CAN-13-0504

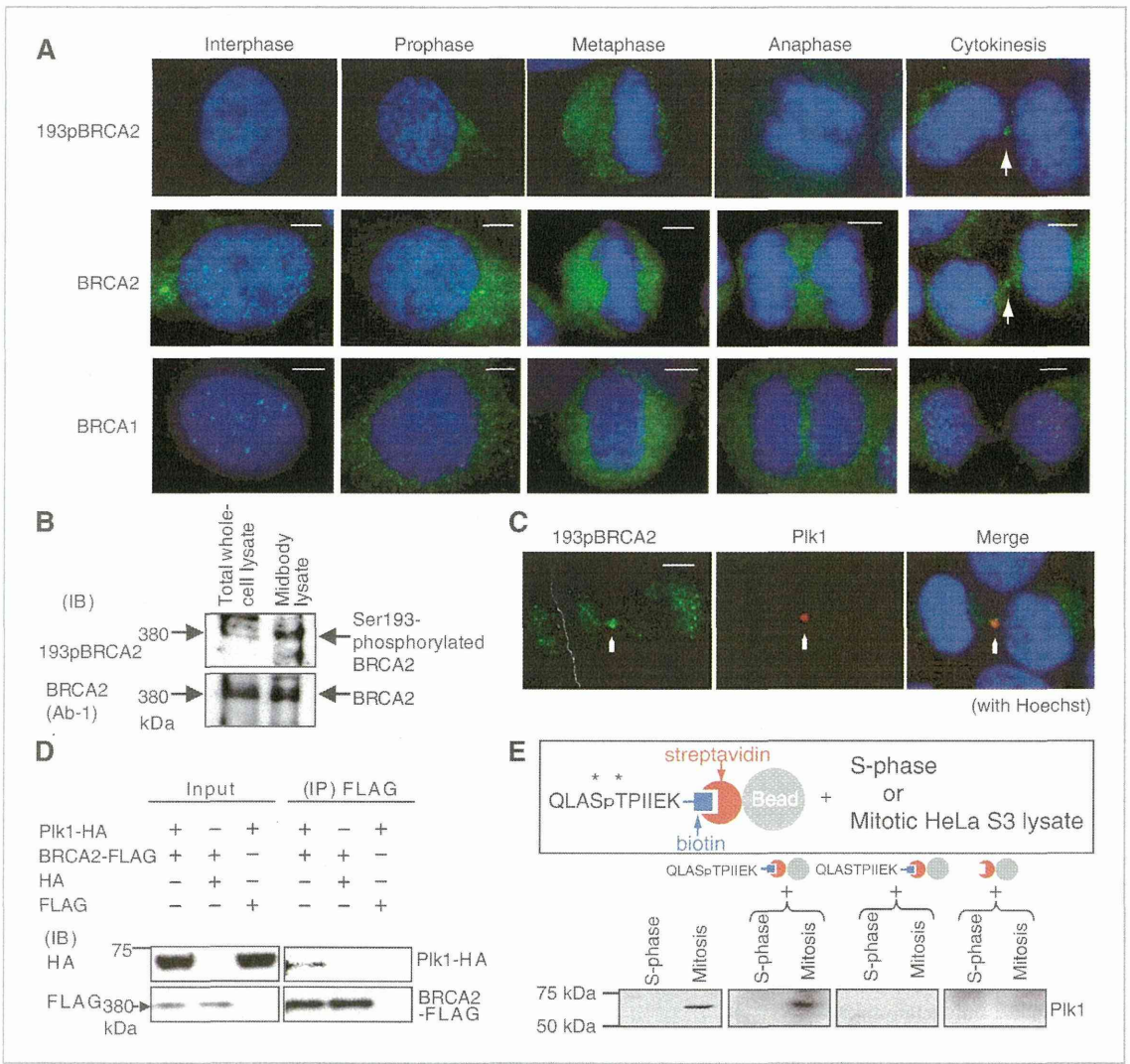

Figure 1. Plk1-phosphorylated BRCA2 localizes to the Flemming body in HeLaS3 cells. A, cells were fixed and stained for Ser193-phosphorylated BRCA2 (pS193-BRCA2), BRCA2, and BRCA1 throughout the cell cycle. Nuclei were detected by Hoechst 33258 stain (blue). Arrows, the Flemming body. Scale bar, 5 μm. B, total whole-cell and midbody lysates were subjected to Western blot analysis using antibodies against pS193-BRCA2 and BRCA2. IB, immunoblot. C, cells were fixed and stained for pS193-BRCA2 (green) and Plk1 (red) in cytokinesis. White arrows, the Flemming body. Scale bar, 5 μm. D, COS-7 cells were transfected with Plk1-HA and/or BRCA2-FLAG expression plasmids. The expression of transgene-derived proteins in input cell lysates and anti-FLAG immunoprecipitates (IP) analyzed using anti-HA or anti-FLAG antibodies are shown. E, N-terminal biotin-fused pThr77 peptides (QLASpTPIIEK) were linked to streptavidin beads and tested for the ability to precipitate Plk1 from S-phase or mitotic HeLaS3 cell lysates. The phosphorylated Thr77 residue and the Ser76 residue crucial for PBD binding are indicated with asterisks (*). Immunoblot analyses show Plk1 coprecipitated with the peptides.

112–685 a.a.] did not affect the localization of the endogenous BRCA2 (Supplementary Fig. S1K). To evaluate further the effect of BRCA2 phosphorylation at Ser193 upon its localization, we expressed either wild-type recombinant BRCA2-FLAG or mutants thereof containing substitutions of Ser193 by alanine (S193A) or glutamate (S193E). Although both the wild-type and the S193E mutant localized to the Flemming body, the S193A mutant did not (Supplementary Fig. S1L). This suggested that phosphorylation of BRCA2 at Ser193 by Plk1 is important for its localization to the Flemming body and that a cancer-associated mutation of BRCA2 might prevent phosphorylation leading to its mislocalization.

Interaction between BRCA2 and NM-IIC

BRCA2 deficiency causes abnormal accumulation of myosin-II, particularly during cytokinesis (6). However, the physiologic role of colocalization of BRCA2 and myosin-II to the midbody remains unclear. We first examined the subcellular

Published OnlineFirst January 21, 2014; DOI: 10.1158/0008-5472.CAN-13-0504

localization of each NM-II isoform in A549 cells during cytokinesis (Fig. 2A). NM-IIC localized to the Flemming body and formed a ring-like structure. In contrast, NM-IIA was diffusively distributed throughout the midbody, and NM-IIB was localized within an area from the basal portion of the midbody to the cytosol of the dividing cell. Similar results were obtained in human mammary epithelial cells (Supplementary Fig. S2A). Further analysis of 3D images by confocal laser microscopy clearly demonstrated that NM-IIC formed part of a unique ring-like structure within the central portion of the midbody (Supplementary Fig. S2B). This structure, which we term the IIC-ring, was approximately 1.5 μm in diameter and colocalized with the Flemming body. To characterize this BRCA2-NM-IIC colocalization further, we analyzed its sedimentation in a glycerol gradient following isolation from A549 cells (Fig. 2B and Supplementary Fig. S2C). The pS193-BRCA2, NM-IIC, Plk1, and MgcRacGAP (a marker of the midbody) were all detected within fraction 2, whereas NM-IIB was detected in fraction 3, and NM-IIA was present in several fractions (1–8). BRCA1 was not found at the midbody and nonphosphorylated BRCA2 was mainly detected within fraction 4 (Supplementary Fig. S2C). These results suggested that pS^{193}-BRCA2 might interact with NM-IIC and MgcRacGAP in addition to Plk1 at the Flemming body. BRCA2-FLAG and NMHC-IIC-HA were coexpressed in COS-7 cells and cell lysates were subjected to immunoprecipitation with anti-FLAG and anti-HA antibodies. NMHC-IIC-HA and BRCA2-FLAG were both detected in the anti-FLAG or anti-HA immunoprecipitates (Fig. 2C). Endogenous BRCA2 immunoprecipitates from A549 cells were shown to contain NMHC-IIC (Fig. 2D and Supplementary Fig. S2D). This result was validated by two different antibodies that recognized distinct epitopes of NMHC-IIC (Fig. 2D) and by mass spectrometric analysis (Supplementary Fig. S2D). Immunoprecipitations from A549 cell lysates using anti-BRCA2 antibody revealed the presence of several protein components in the BRCA2 complex. Polypeptides with apparent molecular weights of 485, 385, 220, 156, and 122 kDa coimmunoprecipitated with BRCA2 (Supplementary Fig. S2D). As a control, we also performed immunoprecipitation with normal rabbit immunoglobulin G (IgG). These polypeptides were digested in gel by trypsin, and the resulting peptides were sequenced by nanoelectrospray mass spectrometry. Besides NMHC-IIC and BRCA2, polycystin-1 (PKD1), ATM, Rho-associated protein kinase 1 (ROCK1), and PARP1 were coimmunoprecipitated by the anti-BRCA2 antibody (Supplementary Fig. S2D). In contrast, NM-IIB did not bind to BRCA2 in this assay. Endogenous MgcRacGAP did not also bind to BRCA2 or NM-IIC (Supplementary Fig. S2E and S2F) despite its colocalization to the Flemming body.

Abnormal cytokinesis following NMHC-IIC gene silencing

To investigate the role of the IIC-ring during cell division, we observed the formation of the midbody 24 hours following siRNA knockdown of NMHC-IIC (Fig. 3A). Midbody structures in most siRNA-control cells were bundled and formed the Flemming bodies (Fig. 3B, top). In contrast, a majority of the cells treated with the NMHC-IIC siRNA retained midbody fibers, that is, exhibited a nonbundled midbody and lacked the Flemming body (Fig. 3B, bottom). The fraction of abnormal cells (exhibiting a non-Flemming body) was 25.2 ± 3.6% in the control cells and 63.5 ± 3.6% in the knockdown cells (Fig. 3B). At 48 hours, we observed a 1.5- to 3-fold increase in the number of multinuclear cells in response to NMHC-IIC knockdown (IIC-1: 57.2 ± 4.5%; IIC-2: 36.3 ± 1.7%) compared with control cells (scrambled control: 21.0 ± 2.0%; no-transfection: 15.8 ± 4.5%; Supplementary Fig. S3A). The NMHC-IIC knockdown cells were observed using time-lapse differential interference microscopy for 48 hours after siRNA treatment. A subpopulation of the cells had fused back together, resulting in binucleated cells. Another subpopulation exhibited catastrophic cell death before cytokinesis completion (Supplementary Fig. S3B). This process is shown in greater detail by time-lapse images (Supplementary Fig. S3C).

Inhibition of IIC-ring formation by BRCA2 gene silencing

To see an effect of BRCA2 suppression on the IIC-ring formation, we silenced BRCA2 using siRNA in A549 cells, which express all three isoforms: IIA, IIB, and IIC (Fig. 3C). As observed in the NMHC-IIC knockdown cells, midbody fibers were present in the absence of the Flemming body in the BRCA2 knockdown cells. Consequently, NM-IIC was distributed throughout the nonbundled midbody, and the IIC-ring was not apparent (Fig. 3D and Supplementary Fig. S3D). A greater number of abnormal midbodies were observed in siRNA-BRCA2–treated cells (siRNA-BRCA2-1: 48.3 ± 2.9%; siRNA-BRCA2-3: 43.3 ± 7.6%) than in control cells (siRNA-luciferase: 21.7 ± 2.9%; no-transfection: 10.0 ± 5.0%; $P = 0.017$; Fig. 3D, right). Similar results were obtained in U2OS cells treated with siRNA targeting BRCA2 (Supplementary Fig. S3E and S3F). To determine whether BRCA2 is important for the formation of midbody structures and progression of cytokinesis, we analyzed the BRCA2 knockdown HeLa S3 cells undergoing cytokinesis. BRCA2 protein levels were reduced after siRNA application (Fig. 3E), and the length of the midbody during cytokinesis in HeLa S3 cells was greater in *BRCA2* siRNA-treated cells than in control cells (siRNA-luciferase or no-transfection: $P < 0.01$; Fig. 3F). Next, we examined whether the length of the midbody in siRNA-BRCA2 cells could be restored by expressing BRCA2-FLAG or BRCA2 (S193A)-FLAG (Supplementary Fig. S3G and S3H). Although BRCA2-FLAG localization was observed in the midbody, this was not seen in BRCA2 (S193A)-FLAG cells (Supplementary Fig. S3H, left). When BRCA2-FLAG was expressed, the length of the midbody was similar to that in the control (siRNA-luciferase). In contrast, the length of the midbody did not recover in cells expressing BRCA2 (S193A)-FLAG ($P = 0.041$; Supplementary Fig. S3H, right), suggesting that it could not localize to the midbody. We did not observe an abnormal midbody or IIC-ring in cells treated with the *BRCA1*-siRNA (Supplementary Fig. S4A–S4E). These results suggest that the formation of the midbody and IIC-ring may require the presence of BRCA2, but not BRCA1, at the Flemming body and that the binding of BRCA2 to NM-IIC is necessary for this process.

Published OnlineFirst January 21, 2014; DOI: 10.1158/0008-5472.CAN-13-0504

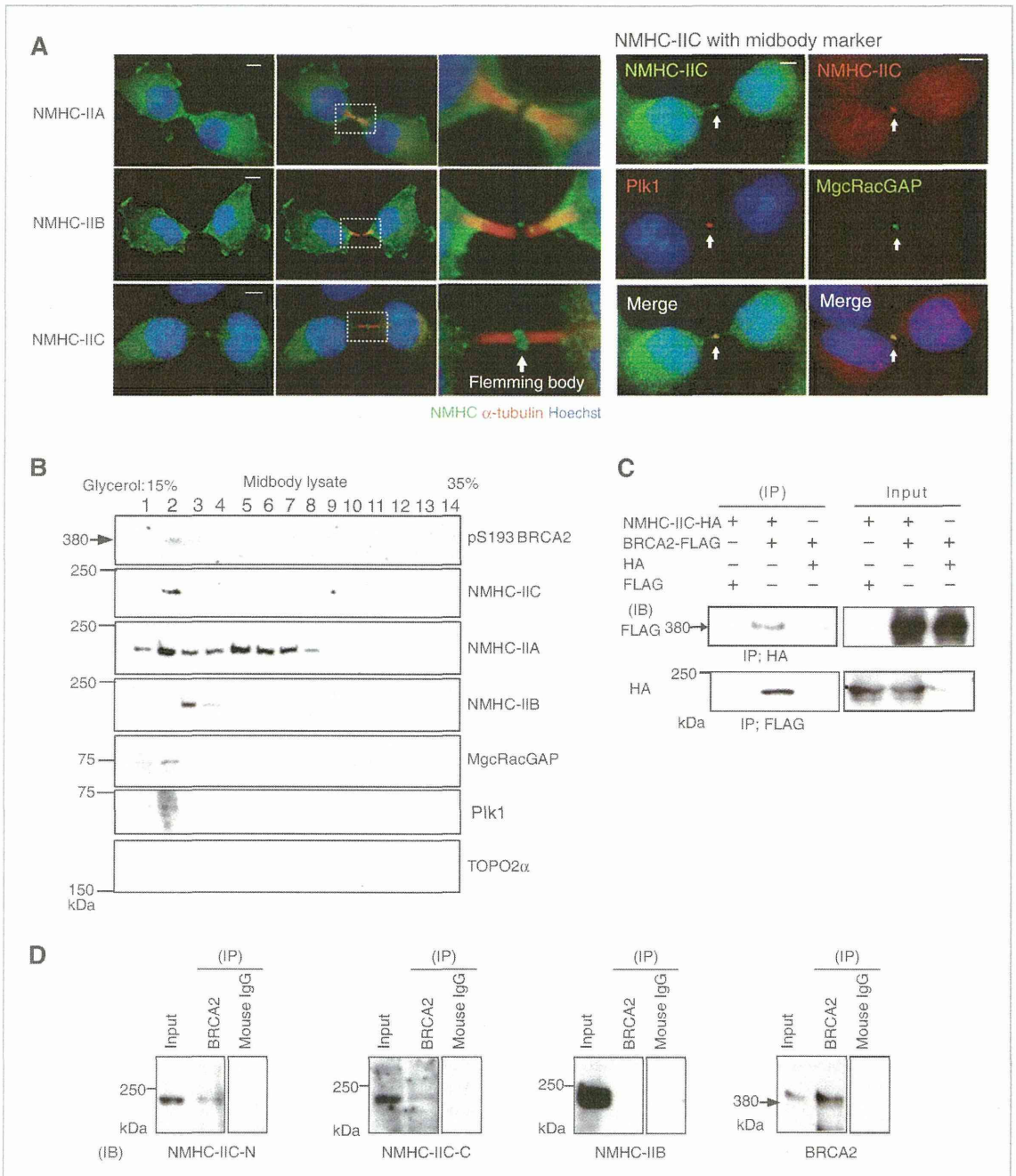

Figure 2. NM-IIC localizes to the Flemming body and interacts with BRCA2. A, immunofluorescence in A549 cells stained for NMHC-IIA (green), IIB (green), IIC (green), and α-tubulin (red). Cells in cytokinesis were also costained for NMHC-IIC (green or red) and Plk1 (red) or MgcRacGAP (green). Scale bar, 5 μm. B, midbody lysates from A549 cells were separated by 15% to 35% (w/v) glycerol gradient centrifugation and subjected to Western blot analysis using the indicated antibodies. The nuclear marker, TOPO2-α, was not detected in any fractions. C, COS-7 cells were transfected with the indicated expression plasmids. The expression of transgene-derived proteins in cell lysates, anti-FLAG immunoprecipitates (IP), and anti-HA immunoprecipitates (IP) revealed by anti-FLAG or anti-HA antibodies are shown. D, A549 cell lysates were immunoprecipitated (IP) with either mouse IgG or anti-BRCA2 antibodies and immunoprecipitates were analyzed using polyclonal antibodies to different epitopes of NMHC-IIC at the N-(NMHC-IIC-N) and C-(NMHC-IIC-C) terminals. Samples were also analyzed by anti-BRCA2 and anti–NMHC-IIB antibodies.

Published OnlineFirst January 21, 2014; DOI: 10.1158/0008-5472.CAN-13-0504

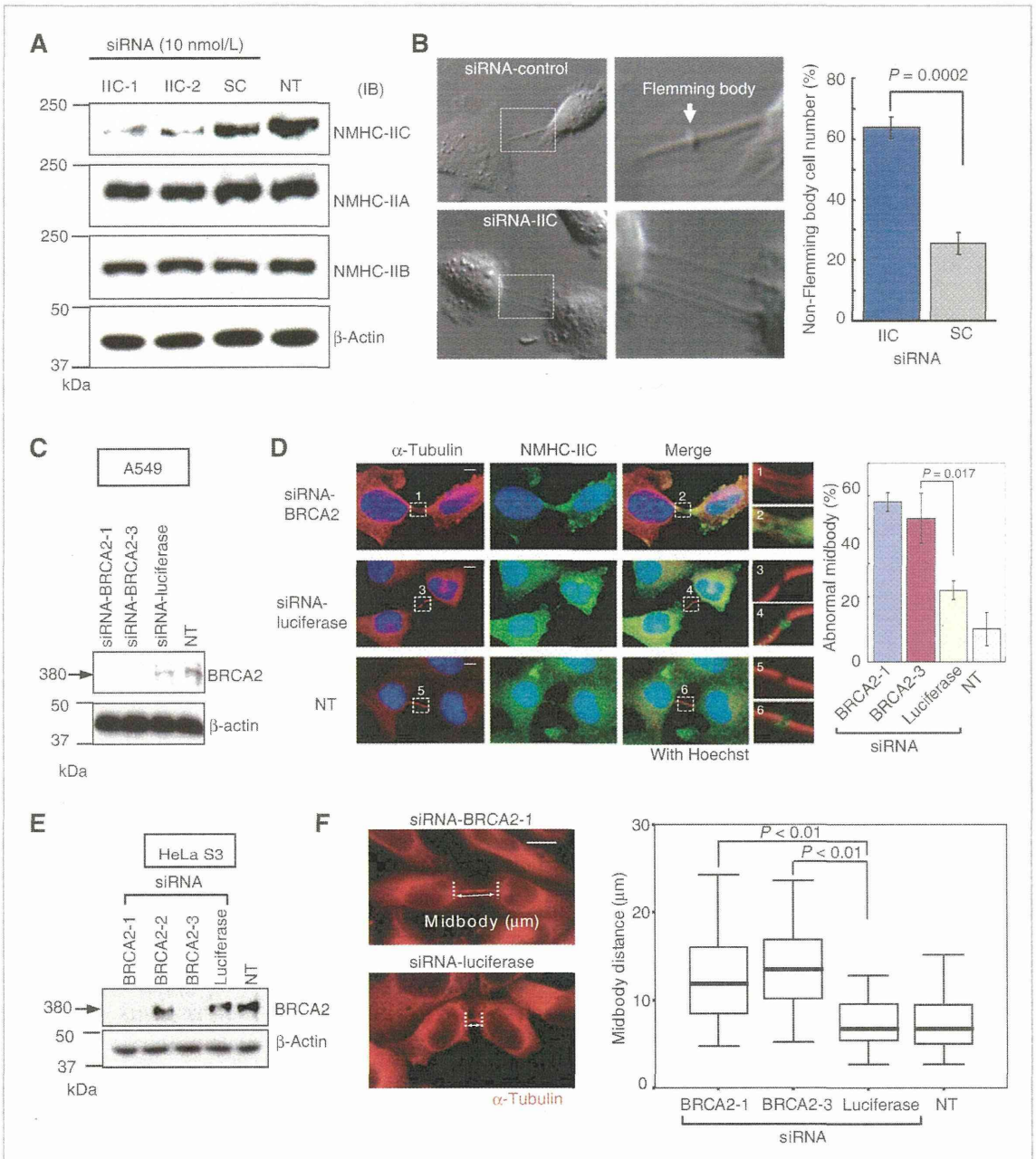

Figure 3. NM-IIC and BRCA2 are essential for midbody formation in A549 cells. A, lysates from A549 cells treated with NMHC-IIC siRNA (IIC-1 or IIC-2) or siRNA-scramble (SC), or no-transfection (NT) were subjected to Western blot analysis using anti–NMHC-IIC, IIA, IIB, and anti–β-actin antibodies. B, NMHC-IIC siRNA (bottom) and siRNA-scramble (top)-treated cells were observed by phase contrast microscopy. The bar graph shows the mean fractions (± SD) of cells showing abnormal midbodies based on three independent experiments ($n = 100$). C, lysates from A549 cells treated with two different BRCA2 siRNAs or siRNA-luciferase or no-transfection (NT) were subjected to Western blot analysis with anti-BRCA2 and anti–β-actin antibodies. D, A549 cells treated with BRCA2 siRNA or siRNA-luciferase or siRNA-no-transfection were fixed and stained with anti–α-tubulin (red) and anti–NMHC-IIC antibodies (green) in cytokinesis. Scale bar, 5 μm. Magnifications of dotted square areas are shown on the right (1–6). The bar graph shows the mean frequencies (±SD) of abnormal midbodies in cells based on three independent experiments ($n = 20$). E, lysates from HeLa S3 cells treated with three different BRCA2 siRNAs or siRNA-luciferase or no-transfection (NT) were subjected to Western blot analysis with anti-BRCA2 and anti–β-actin antibodies. F, HeLa S3 cells treated with BRCA2 siRNA (BRCA2-1) were fixed and stained for α-tubulin (red). White lines, the measured midbody length by Adobe Photoshop CS3 software. Scale bar, 5 μm. The midbody lengths are shown in box plot that signifies the top and bottom quartiles. The medians are represented by bold lines. Nonparametric data were statistically analyzed by the Mann–Whitney *U* test ($n = 81$ in each case, $P < 0.01$).

Published OnlineFirst January 21, 2014; DOI: 10.1158/0008-5472.CAN-13-0504

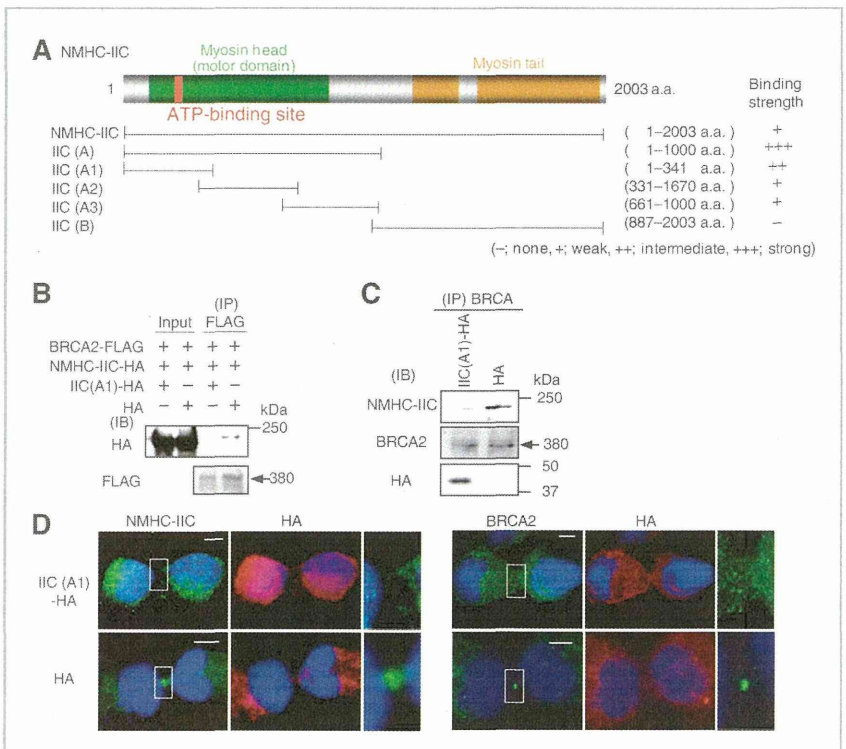

Figure 4. The binding inhibition between BRCA2 and NM-IIC affects the formation of Flemming body. A, a schematic diagram of NMHC-IIC deletion mutants [IIC (A), (B), (A1), (A2), and (A3)] and the strength of binding to BRCA2, summarizing the data within Supplementary Fig. S5A and S5B. NMHC-IIC fragments were fused to an HA tag. B, COS-7 cells transfected with indicated plasmids were lysed and proteins were immunoprecipitated with anti-FLAG antibody. Inputs and precipitates (IP) were visualized by anti-HA and anti-FLAG antibodies. C, A549 cells were transfected with either IIC (A1)-HA or HA and midbodies were collected. Anti-BRCA2 immunoprecipitates (IP) from midbody lysates were analyzed by anti–NMHC-IIC, anti-BRCA2, and anti-HA antibodies. D, A549 cells were transfected with IIC (A1)-HA or HA and stained with anti–NMHC-IIC (green) or BRCA2 (green), and anti-HA (red) antibodies. Scale bar, 5 μm.

Binding of BRCA2 to the N-terminal region of NMHC-IIC

To determine which region of NMHC-IIC interacts with BRCA2, we introduced plasmids encoding HA-tagged NMHC-IIC deletion mutants (Fig. 4A) and BRCA2-FLAG into COS-7 cells, and performed coimmunoprecipitation analyses. BRCA2 bound to the IIC (A)-HA fusion, containing a.a. 1–1,000 of NMHC-IIC (Supplementary Fig. S5A). We further divided this fragment into three partially overlapping regions and found that only the IIC (A1)-HA fusion bound strongly to BRCA2-FLAG (Supplementary Fig. S5B). When IIC (A1)-HA was coexpressed with BRCA2-FLAG and NMHC-IIC-HA, the interaction between BRCA2-FLAG and NMHC-IIC-HA was abolished (Fig. 4B). The same dominant-negative effect was seen between the endogenous BRCA2 and NM-IIC at the midbody (Fig. 4C). Both the localization of endogenous BRCA2 and IIC-ring formation at the Flemming body were disrupted in A549 cells expressing IIC (A1)-HA (Fig. 4D and Supplementary Fig. S5C).

Abnormalities in cytokinesis induced by expression of NMHC-IIC (A1) or BRCA2 (R1)

We hypothesized that the interaction between BRCA2 and NM-IIC at the midbody might play a role in the regulation of cytokinesis. To explore this possibility, we analyzed A549 cells exposed to anti–α-tubulin antibody 48 hours after IIC (A1)-HA transfection. The midbodies of the IIC (A1)-HA–expressing cells varied in length compared with those of the HA-expressing control cells (Supplementary Fig. S5D; $P < 0.01$ by Mann–Whitney U test). The IIC (A1)-HA–expressing cells were unable to divide and accumulated at G_1 phase (76.09%–48.89% for the cells transfected with the empty vector; Supplementary Fig. S5E). These results indicated that the binding of BRCA2 to NM-IIC could have a function in cytokinesis promotion.

Because the endogenous BRCA2 did not localize to the Flemming body in A549 cells expressing the R1 region of BRCA2 (Supplementary Fig. S1K), we supposed that the abundant expression of the R1 domain would also inhibit IIC-ring formation. As expected, the IIC ring was not observed in A549 cells expressing a high level of HA-BRCA2 (R1), as was the case in cells expressing IIC (A1)-HA (Fig. 4D and Supplementary Fig. S5C and S5F). A greater number of binucleated cells was observed in BRCA2 (R1)-FLAG–expressing cells (18.5 ± 3.4%) than in FLAG-expressing control cells (8.3 ± 2.7%; Supplementary Fig. S5G).

Enhancement of the ATPase activity of NM-IIC by BRCA2

NM-II plays a fundamental role in cell adhesion, migration, and division mediated by inherent actin cross-linking and contractile functions. This activity requires energy, which is provided by the hydrolysis of ATP and the active site of NM-II exhibits ATPase activity. Treatment of A549 cells with blebbistatin, an inhibitor of myosin II ATPase activity, caused decay of the IIC-ring surrounding α-tubulin and imperfections in ring formation (Supplementary Fig. S6A). MgcRacGAP was observed in the decay of the IIC-ring (Supplementary Fig.

Published OnlineFirst January 21, 2014; DOI: 10.1158/0008-5472.CAN-13-0504

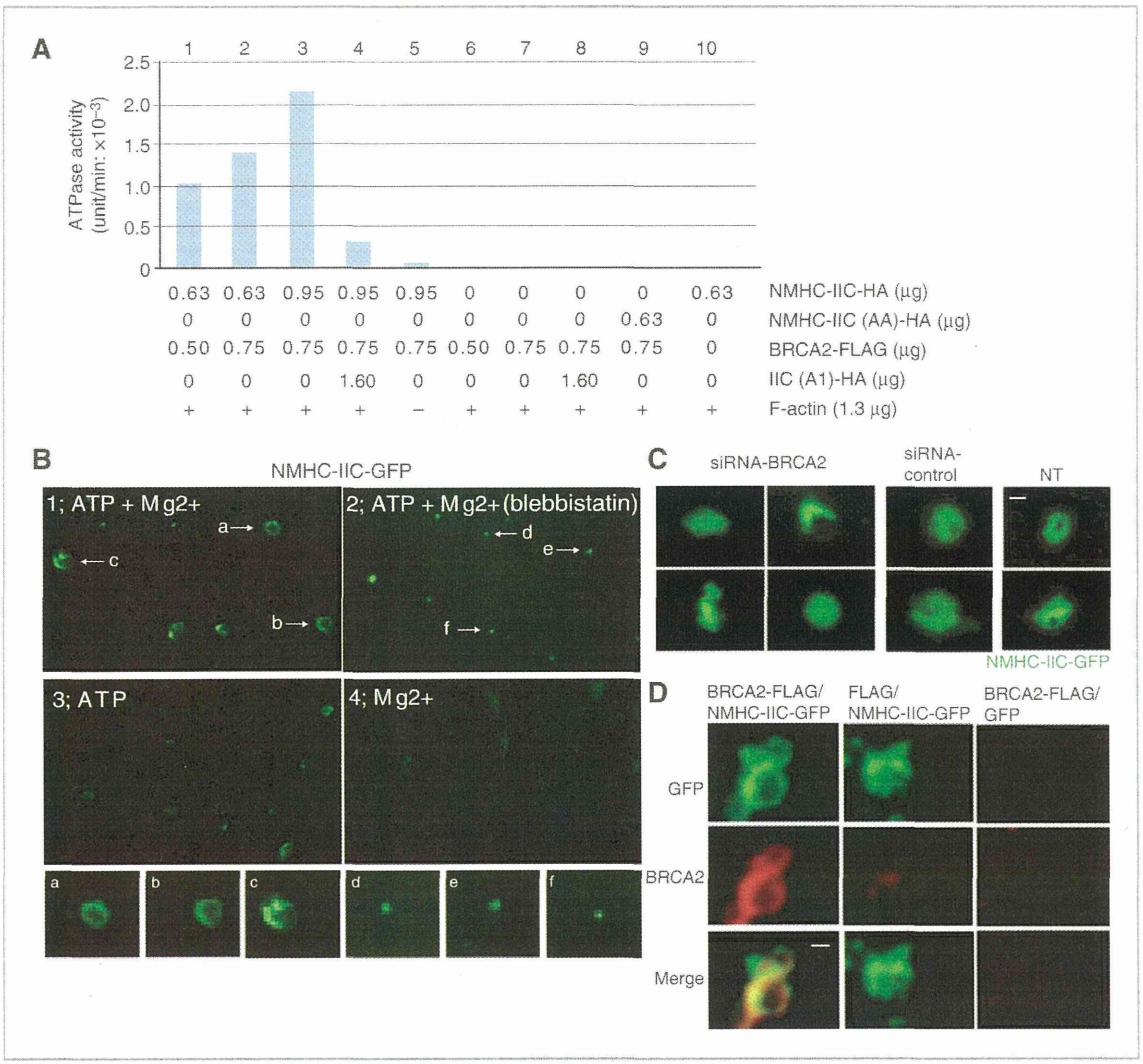

Figure 5. ATPase activity is required for IIC-ring formation. A, the actin-dependent ATPase activity of NM-IIC following incubation of the immunoprecipitated NMHC-IIC-HA with and without BRCA2-FLAG. B, NMHC-IIC-GFP was expressed in COS-7 cells and the reaction mixtures were mounted on a glass slide and observed by fluorescence microscopy. The IIC-rings were not seen following blebbistatin treatment or lacking either ATP or Mg2+ in the reaction. Magnified images of NMHC-IIC-GFP are also shown (a–f). C, NMHC-IIC-GFP was expressed in COS-7 cells treated with siRNA-BRCA2 or siRNA-control or no-transfection, and the reaction mixtures were mounted on a glass slide and observed by fluorescence microscopy. The samples were fixed and stained for GFP (green). Scale bar, 1 μm. D, the plasmids indicated in figure were expressed in COS-7 cells and the cell lysates were mounted on a glass slide. The samples were fixed and stained for GFP (green) and BRCA2 (red). Scale bar, 1 μm.

S6B). To explore the function of BRCA2 in IIC-ring formation, we analyzed the effect of BRCA2 on the actin-dependent ATPase activity of NM-IIC. The actin-dependent ATPase activity of NM-IIC was measured following incubation of the immunoprecipitated NMHC-IIC-HA in the presence or absence of BRCA2-FLAG. We confirmed that introduction of the plasmid encoding NMHC-IIC into cells leads to binding of the exogenous NMHC-IIC to the 12A and 12B isoforms of endogenous light chain (Supplementary Fig. S6C). The ATPase was activated (1.0×10^{-3} unit/minute) when both proteins were present (0.5 μg BRCA2-FLAG and 0.63 μg NMHC-IIC-HA; Fig. 5A, lane 1). ATPase activation following incubation of NMHC-IIC and BRCA2 occurred in a dose-dependent manner (Fig. 5A, lanes 1 and 2). The light chain was phosphorylated following the addition of BRCA2-FLAG to the immunoprecipitated NMHC-IIC (Supplementary Fig. S6D). Furthermore, in the presence of IIC (A1)-HA, which inhibits the binding of BRCA2 to NM-IIC, ATPase activation was inhibited (Fig. 5A, lane 4). The absence of F-actin from the reaction mixture reduced ATPase activity significantly (Fig. 5A, lane 5). The

Published OnlineFirst January 21, 2014; DOI: 10.1158/0008-5472.CAN-13-0504

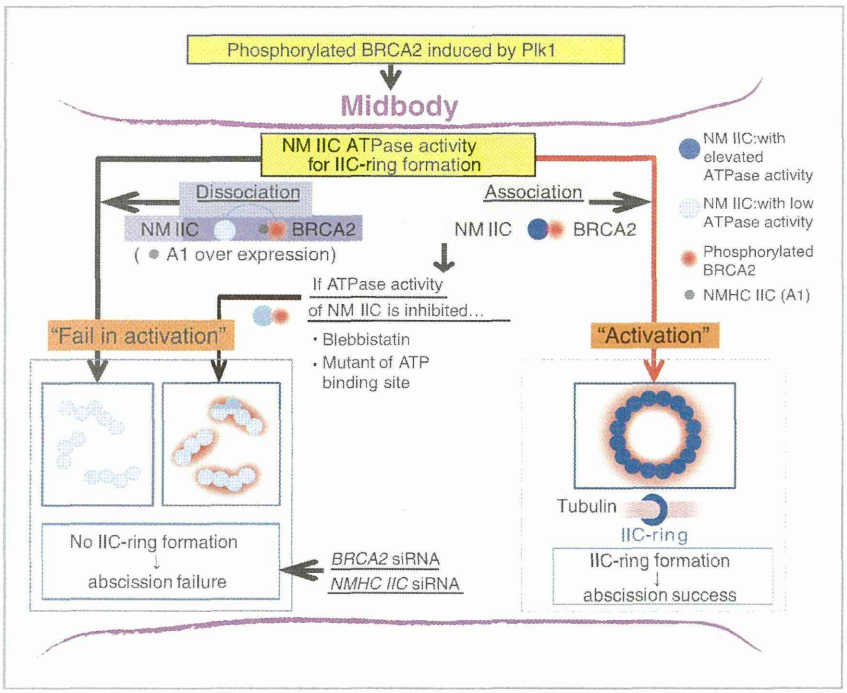

Figure 6. The midbody abscission is modulated by the BRCA2–NM-IIC complex. The phosphorylation of BRCA2 by Plk1 is required for BRCA2 localization to the Flemming body and may support IIC-ring formation through increased NM-IIC-ATPase activity. When BRCA2-NM-IIC binding inhibition induced by IIC (A1) overexpression, the activation of NM-IIC ATPase failed and the IIC-ring was not formed normally as it would be with treatment with blebbistatin (ATPase inhibitor of myosin) to the cells. The IIC-ring is triggered by BRCA2-dependent binding of NM-IIC at the Flemming body, which may allow BRCA2 to modulate the midbody abscission for normal transition of cells through cytokinesis.

localization of F-actin at the Flemming body was observed by immunofluorescence microscopy (Supplementary Fig. S6E). A mutant NMHC-IIC (AA)-HA in which Lys204 and Thr205 in the ATP-binding site (GESGAGKT; 198–205) were substituted with alanine did not exhibit ATPase activity in response to incubation with BRCA2 (Fig. 5A, lane 9). IIC (A1)-HA also did not exhibit ATPase activity (Fig. 5A, lane 8). A mutant BRCA2 (S193A)-FLAG also supported activation of NM-IIC ATPase activity to a level similar to that observed by the wild-type BRCA2-FLAG (Supplementary Fig. S6F). These results suggested that the ATPase activity is increased by NM-IIC–BRCA2 association. Furthermore, the phosphorylation of BRCA2-Ser193 is not essential for the activation of the ATPase activity of NM-IIC but is required for the localization of BRCA2 to the Flemming body.

To test this further, we attempted an *in vitro* reconstitution of the IIC-ring using recombinant NMHC-IIC. NMHC-IIC-GFP was expressed in COS-7 cells and examined using the cell lysates. It was observed that NMHC-IIC-GFP formed part of a unique ring-like structure (1.4–2.0 μm) in the presence of both ATP and Mg^{2+} (Fig. 5B, 1). However, NMHC-IIC-GFP failed to organize into a ring-like structure when blebbistatin was added to the reaction (Fig. 5B, 2). The ring-like structure was also not observed in the absence of either ATP or Mg^{2+} (Fig. 5B, 3 and 4). To see an effect of BRCA2 on IIC-ring formation, we overexpressed NMHC-IIC-GFP following siRNA-mediated knockdown of BRCA2 in COS-7 cells. NMHC-IIC-GFP failed to organize into a ring-like structure in siRNA-BRCA2–treated cells (Fig. 5C). Next, we coexpressed recombinant NMHC-IIC-GFP and BRCA2-FLAG in COS-7 cells and investigated localization of BRCA2 in the lysates. We showed that BRCA2 localized to the IIC ring-like structure (Fig. 5D). These results suggest that the ring-like structure is composed of NMHC-IIC-GFP and BRCA2.

The requirement of the ATPase activity of NM-IIC for IIC-ring formation

To demonstrate the significance of the ATPase activity of NM-IIC for IIC ring formation, we examined whether the IIC-ring could be restored by recombinant NMHC-IIC-HA or NMHC-IIC (AA)-HA expression following endogenous NMHC-IIC knockdown (Supplementary Fig. S6G and S6H). Both were coprecipitated with BRCA2-FLAG (Supplementary Fig. S6I). Although cells expressing wild-type NMHC-IIC-HA exhibited IIC-ring within the midbody, in cells expressing NMHC-IIC (AA)-HA, the IIC-ring-like structure seemed to degenerate within the midbody area (Supplementary Fig. S6J). These results indicate that the ATPase activity of NM-IIC is required for IIC-ring formation.

Discussion

BRCA2, the product of breast cancer susceptibility gene *BRCA2*, plays important roles in the maintenance of genome stability throughout the cell cycle. Several studies have suggested a role for BRCA2 in regulation of cytokinesis at the late M phase. BRCA2 deficiency impairs completion of cell division. Inhibition of cell separation is accompanied by abnormalities in NM-II organization during the late stages of cytokinesis (6). We identified the subcellular localization of each isoform

Published OnlineFirst January 21, 2014; DOI: 10.1158/0008-5472.CAN-13-0504

during cytokinesis and found that only the NM-IIC isoform colocalizes and interacts with BRCA2 at the Flemming body (Fig. 2 and Supplementary Fig. S2). The interaction of NM-IIC with BRCA2 at the Flemming body allows the activation of NM-IIC ATPase activity followed by IIC-ring formation (Fig. 6).

Cytokinesis, the final step of cell division in all animal cells, partitions the cytoplasm between two daughter cells. This process depends upon the activity of NM-II, which participates in the formation of the cleavage furrow. Attachment of a contractile ring, consisting of a network of actin filaments (actomyosin) and NM-II, to the cytoplasmic membrane induces the formation of a cleavage furrow. Mammalian cells use not IIC but IIA or IIB during this process (10). NM-IIA exhibited a diffuse distribution throughout the entire midbody as observed by immunofluorescence microscopy (Fig. 2A) and glycerol gradient analyses (Fig. 2B), indicating that it might interact with various proteins. Although NM-IIB localizes to an area from the basal portion of the midbody to the cytosol of dividing cells, glycerol gradient analysis revealed that it is absent from the fraction containing phosphorylated BRCA2. In addition, a coimmunoprecipitation assay did not detect interaction between BRCA2 and NM-IIB (Fig. 2D). In contrast, NM-IIC was detected at the Flemming body and it colocalized with phosphorylated BRCA2 during cytokinesis just before abscission. Depletion of BRCA2 or NM-IIC by siRNA disrupted the IIC-ring and led to abnormal midbody formation followed by failure of abscission and cytokinesis (Fig. 3 and Supplementary Fig. S3). Cells expressing NM-IIC (A1), which exhibited a dominant-negative effect upon the interaction of endogenous BRCA2 and NM-IIC, also failed to progress through cytokinesis (Fig. 4 and Supplementary Fig. S5C–S5E). Taken together, the interaction between BRCA2 and NM-IIC seems essential for abscission or the induction thereof. Some cells, including HeLa S3, have been reported not to express NM-IIC; however, we have performed some experiments to confirm NM-IIC-expression in HeLa S3 cells. These include Western blot data using anti–NMHC-IIC-N antibody and the mass spectrometric analysis of HeLa S3-cell lysates (data not shown). These data indicated the existence of the short type of NM-IIC in HeLa S3 cells.

In this study, the interaction of BRCA2 with NM-IIC was shown to be required for the activation of NM-IIC ATPase activity (Fig. 5A and Supplementary Fig. S6F). Furthermore, the endogenous light chain bound to NMHC-IIC-HA was phosphorylated following the addition of BRCA2-FLAG (Supplementary Fig. S6C and S6D). We speculate that a kinase present in the BRCA2 immunoprecipitate might phosphorylate the light chain, resulting in the activation of ATPase activity. ROCK, which phosphorylates Ser19 of smooth muscle MLC2, was detected in the anti-BRCA2 immunoprecipitates by mass spectrometry. This result raises the possibility that ROCK1 may phosphorylate and activate myosin IIC. This issue should be addressed in future studies.

BRCA2 is a multifunctional protein that functions as a caretaker of genome stability throughout the cell cycle, including during processes such as DNA synthesis, centrosome dynamics, chromosome separation, and cytokinesis. In this study, we demonstrated a role for BRCA2 in the late stage of cytokinesis in collaboration with NM-IIC, which should help clarify the mechanics of cytokinesis and breast oncogenesis. We identified in the BIC database a missense mutation in BRCA2 (T77A, within the Plk1-binding motif), the clinical significance of which had not been established. We showed the possibility that this mutation may abolish the binding between BRCA2 and Plk1, resulting in failure of BRCA2 localization to the Flemming body and cytokinesis incompletion, suggesting that this mutation may underlie the development of breast cancer.

Disclosure of Potential Conflicts of Interest

No potential conflicts of interest were disclosed.

Authors' Contributions

Conception and design: Y. Miki, A. Nakanishi
Development of methodology: M. Takaoka, Y. Miki, A. Nakanishi
Acquisition of data (provided animals, acquired and managed patients, provided facilities, etc.): M. Takaoka, A. Nakanishi
Analysis and interpretation of data (e.g., statistical analysis, biostatistics, computational analysis): M. Takaoka, A. Nakanishi
Writing, review, and/or revision of the manuscript: M. Takaoka, K. Takenaka, Y. Miki, A. Nakanishi
Administrative, technical, or material support (i.e., reporting or organizing data, constructing databases): M. Takaoka, H. Saito, Y. Miki, A. Nakanishi
Study supervision: K. Takenaka, c, A. Nakanishi

Acknowledgments

The authors thank Rie Hayashi (Leica Microsystems K.K.) for support in preparing the laser-scanning confocal microscope.

Grant Support

This work was supported by JSPS KAKENHI Grant Numbers 24300328 (Y. Miki), 25640061 (Y. Miki), 21790311 (K. Takenaka), 23590355 (K. Takenaka), by Ishidsu Shun Memorial Scholarship (M. Takaoka), and by Takeda Science Foundation (K. Takenaka).

The costs of publication of this article were defrayed in part by the payment of page charges. This article must therefore be hereby marked *advertisement* in accordance with 18 U.S.C. Section 1734 solely to indicate this fact.

Received February 18, 2013; revised December 20, 2013; accepted January 5, 2014; published OnlineFirst January 21, 2014.

References

1. Moynahan ME, Pierce AJ, Jasin M. BRCA2 is required for homology-directed repair of chromosomal breaks. Mol Cell 2001;7:263–72.
2. Wong AK, Pero R, Ormonde PA, Tavtigian SV, Bartel PL. RAD51 interacts with the evolutionarily conserved BRC motifs in the human breast cancer susceptibility gene brca2. J Biol Chem 1997;272:31941–4.
3. Chen PL, Chen CF, Chen Y, Xiao J, Sharp ZD, Lee WH, et al. The BRC repeats in BRCA2 are critical for RAD51 binding and resistance to methyl methanesulfonate treatment. Proc Natl Acad Sci U S A 1998;95:5287–92.
4. Tutt A, Gabriel A, Bertwistle D, Connor F, Paterson H, Peacock J, et al. Absence of Brca2 causes genome instability by chromosome breakage and loss associated with centrosome amplification. Curr Biol 1999;9:1107–10.
5. Nakanishi A, Han X, Saito H, Taguchi K, Ohta Y, Imajoh-Ohmi S, et al. Interference with BRCA2, which localizes to the centrosome during S

Published OnlineFirst January 21, 2014; DOI: 10.1158/0008-5472.CAN-13-0504

and early M phase, leads to abnormal nuclear division. Biochem Biophys Res Commun 2007;355:34–40.
6. Daniels MJ, Wang Y, Lee M, Venkitaraman AR. Abnormal cytokinesis in cells deficient in the breast cancer susceptibility protein BRCA2. Science 2004;306:876–9.
7. Jonsdottir AB, Vreeswijk MP, Wolterbeek R, Devilee P, Tanke HJ, Eyfjord JE, et al. BRCA2 heterozygosity delays cytokinesis in primary human fibroblasts. Cell Oncol 2009;31:191–201.
8. Dean SO, Rogers SL, Stuurman N, Vale RD, Spudich JA. Distinct pathways control recruitment and maintenance of myosin II at the cleavage furrow during cytokinesis. Proc Natl Acad Sci U S A 2005;102:13473–8.
9. Reichl EM, Ren Y, Morphew MK, Delannoy M, Effler JC, Girard KD, et al. Interactions between myosin and actin crosslinkers control cytokinesis contractility dynamics and mechanics. Curr Biol 2008; 18:471–80.
10. Beach JR, Egelhoff TT. Myosin II recruitment during cytokinesis independent of centralspindlin-mediated phosphorylation. J Biol Chem 2009;284:27377–83.
11. Gromley A, Yeaman C, Rosa J, Redick S, Chen CT, Mirabelle S, et al. Centriolin anchoring of exocyst and SNARE complexes at the midbody is required for secretory-vesicle-mediated abscission. Cell 2005; 123:75–87.
12. Lee M, Daniels MJ, Garnett MJ, Venkitaraman AR. A mitotic function for the high-mobility group protein HMG20b regulated by its interaction with the BRC repeats of the BRCA2 tumor suppressor. Oncogene 2011;30:3360–9.
13. Ryser S, Dizin E, Jefford CE, Delaval B, Gagos S, Christodoulidou A, et al. Distinct roles of BARD1 isoforms in mitosis: full-length BARD1 mediates aurora B degradation, cancer-associated BARD1beta scaffolds aurora B and BRCA2. Cancer Res 2009;69: 1125–34.
14. Mondal G, Rowley M, Guidugli L, Wu J, Pankratz VS, Couch FJ, et al. BRCA2 localization to the midbody by filamin A regulates CEP55 signaling and completion of cytokinesis. Dev Cell 2012;23:137–52.
15. Elia AE, Cantley LC, Yaffe MB. Proteomic screen finds pSer/pThr-binding domain localizing Plk1 to mitotic substrates. Science 2003;299:1228–31.
16. Barr FA, Sillje HH, Nigg EA. Polo-like kinases and the orchestration of cell division. Nat Rev Mol Cell Biol 2004;5:429–40.
17. van de Weerdt BC, Littler DR, Klompmaker R, Huseinovic A, Fish A, Perrakis A, et al. Polo-box domains confer target specificity to the polo-like kinase family. Biochim Biophys Acta 2008;1783:1015–22.
18. Negishi T, Kumano G, Nishida H. Polo-like kinase 1 is required for localization of posterior end mark protein to the centrosome-attracting body and unequal cleavages in ascidian embryos. Dev Growth Differ 2011;53:76–87.
19. Lin HR, Ting NS, Qin J, Lee WH. M phase-specific phosphorylation of BRCA2 by polo-like kinase 1 correlates with the dissociation of the BRCA2-P/CAF complex. J Biol Chem 2003;278:35979–87.
20. Lee M, Daniels MJ, Venkitaraman AR. Phosphorylation of BRCA2 by the polo-like kinase Plk1 is regulated by DNA damage and mitotic progression. Oncogene 2004;23:865–72.
21. Leal A, Endele S, Stengel C, Huehne K, Loetterle J, Barrantes R, et al. A novel myosin heavy chain gene in human chromosome 19q13.3. Gene 2003;312:165–71.
22. Golomb E, Ma X, Jana SS, Preston YA, Kawamoto S, Shoham NG, et al. Identification and characterization of nonmuscle myosin II-C, a new member of the myosin II family. J Biol Chem 2004;279:2800–8.
23. Fujita-Becker S, Tsiavaliaris G, Ohkura R, Shimada T, Manstein DJ, Sutoh K. Functional characterization of the N-terminal region of myosin-2. J Biol Chem 2006;281:36102–9.
24. van Duffelen M, Chrin LR, Berger CL. Kinetics of structural changes in the relay loop and SH3 domain of myosin. Biochem Biophys Res Commun 2005;329:563–72.
25. Jana SS, Kawamoto S, Adelstein RS. A specific isoform of nonmuscle myosin II-C is required for cytokinesis in a tumor cell line. J Biol Chem 2006;281:24662–70.
26. Mullins JM, McIntosh JR. Isolation and initial characterization of the mammalian midbody. J Cell Biol 1982;94:654–61.